Diagn Interv Radiol 2026; DOI: 10.4274/dir.2025.253590

INTERVENTIONAL RADIOLOGY

ORIGINAL ARTICLE

Diagnostic performance of magnetic resonance imaging-targeted biopsy for PI-RADS ≥3 peripheral zone lesions in multiparametric prostate magnetic resonance imaging: correlation with clinically significant prostate cancer

Serdar Aslan[1],
Emrah Sülün[1],
Ertuğrul Çakır[1],
Ural Oğuz[2],
Tümay Bekçi[1]

[1]Giresun University Faculty of Medicine, Department of Radiology, Giresun, Türkiye

[2]Giresun University Faculty of Medicine, Department of Urology, Giresun, Türkiye

Corresponding author: Serdar Aslan

E-mail: serdaraslan28@hotmail.com

Received 31 July 2025; revision requested 08 September 2025; last revision received 13 October 2025; accepted 15 October 2025.

Epub: 03.11.2025

Publication date: 04.05.2026

DOI: 10.4274/dir.2025.253590

PURPOSE

To evaluate magnetic resonance imaging (MRI)-targeted biopsy (MRI-TB) performance in detecting clinically significant prostate cancer (csPCa) with a Prostate Imaging Reporting and Data System (PI-RADS) score of ≥3 peripheral zone (PZ) lesions using multiparametric MRI (mpMRI)-histopathology correlation.

METHODS

This retrospective study included 141 patients with 187 PZ lesions who underwent mpMRI followed by both MRI-TB and transrectal ultrasound-guided systematic biopsy (SB) between December 2021 and December 2024. All mpMRI scans were evaluated by a board-certified experienced radiologist in accordance with the PI-RADS version 2.1 criteria. The csPCa detection rates of SB, MRI-TB, and combined biopsy (CB) were compared. Statistical analyses included McNemar's test, Fisher's exact test, and the Mann–Whitney U test. A *P* value <0.05 was considered statistically significant.

RESULTS

Among the 141 patients (187 PI-RADS ≥3 PZ lesions), patients with csPCa exhibited significantly higher prostate-specific antigen (PSA) levels (15.3 vs. 8.2 ng/mL; $P = 0.02$), lower prostate volume (52.4 vs. 78.6 mL; $P < 0.001$), and three-fold higher PSA density (PSAD) (0.30 vs. 0.10 ng/mL/mL; $P < 0.001$) than non-csPCa cases. Notably, PSAD > 0.15 ng/mL/mL occurred in 78% of patients with csPCa vs. 18% in non-csPCa cases ($P < 0.001$). Moreover, MRI-TB detected significantly more csPCa than SB (17.7% vs. 10.7% of lesions; $P < 0.001$), with maximal advantage in PI-RADS 4 lesions (20.7% vs. 10.9%; $P = 0.004$). By contrast, CB did not significantly increase csPCa detection over MRI-TB alone (19.8% vs. 17.7%; $P = 0.125$). Chronic prostatitis (CP) (34.0% of benign cases) confounded PI-RADS specificity.

CONCLUSION

For csPCa detection in PI-RADS ≥3 PZ lesions, particularly PI-RADS 4, MRI-TB outperforms SB. For PI-RADS 5, SB and MRI-TB showed equivalent efficacy. However, MRI-TB alone suffices for PI-RADS ≥4 lesions or PSAD >0.15 ng/mL/mL, whereas CB remains preferable for PI-RADS 3. The high CP prevalence underscores the need for adjunctive biomarkers to improve specificity.

CLINICAL SIGNIFICANCE

MRI-TB optimizes csPCa detection for PI-RADS ≥4 PZ lesions, reducing reliance on SBs. A PSAD threshold >0.15 ng/mL/mL effectively stratifies biopsy necessity, and high CP prevalence (34% of benign cases) underscores the need for adjunct biomarkers to improve specificity in PI-RADS 3–4 lesions.

KEYWORDS

Magnetic resonance imaging-targeted biopsy, Prostate Imaging Reporting and Data System, peripheral zone, magnetic resonance imaging

You may cite this article as: Aslan S, Sülün E, Çakır E, Oğuz U, Bekçi T. Diagnostic performance of magnetic resonance imaging-targeted biopsy for PI-RADS ≥3 peripheral zone lesions in multiparametric prostate magnetic resonance imaging: correlation with clinically significant prostate cancer. *Diagn Interv Radiol*. 2026;32(3):328-337.

Prostate cancer (PCa) ranks as the second most frequently diagnosed malignancy in men worldwide and the seventh leading cause of cancer-related death.[1] Approximately 95% of PCas are adenocarcinomas arising from glandular epithelial cells, predominantly in the peripheral zone (PZ), whereas approximately 25% originate in the transitional zone (TZ); rare cases involve neuroendocrine, basal cell, or mesenchymal tumors.[2,3]

The incidence of PCa increases substantially with age, predominantly affecting men over 65 years, with family history serving as a well-established risk factor, particularly when first-degree relatives are diagnosed before the age of 65.[1,4] Early-stage PCa often remains asymptomatic but may present with metastatic symptoms in advanced disease, emphasizing the importance of early detection to reduce morbidity and mortality.

The prostate-specific antigen (PSA) test remains the primary screening tool, although its specificity is limited by frequent elevation in benign conditions, such as benign prostatic hyperplasia (BPH) and prostatitis.[5] PSA density (PSAD), calculated by dividing the PSA level by the prostate volume, enhances diagnostic accuracy when combined with age, percent-free PSA, and family history.[6,7]

Main points

- Magnetic resonance imaging-targeted biopsy (MRI-TB) outperforms systematic biopsy (SB) in detecting clinically significant prostate cancer (csPCa) with a Prostate Imaging Reporting and Data System (PI-RADS) score ≥3 peripheral zone lesions (17.7% vs. 10.7%; $P < 0.001$), with maximal advantage in PI-RADS 4 lesions (20.7% vs. 10.9%; $P = 0.004$).
- Chronic prostatitis confounds PI-RADS specificity, present in 34% of benign cases and mimicking csPCa on multiparametric MRI, particularly in PI-RADS 3–4 lesions.
- Prostate-specific antigen density (PSAD) >0.15 ng/mL/mL is a robust predictor of csPCa (78% sensitivity) and reduces unnecessary biopsies in equivocal lesions.
- Combined biopsy did not significantly increase csPCa detection over MRI-TB alone (19.8% vs. 17.7%; $P = 0.125$), supporting MRI-TB as a first-line intervention for PI-RADS ≥4 or high PSAD.
- SB remains viable for PI-RADS 5 lesions (equivalent csPCa detection to MRI-TB: 18.5% each), optimizing resource use in high-volume settings.

Transrectal ultrasound (TRUS)-guided systematic biopsy (SB), typically involving 12-core sampling, is the standard diagnostic technique. However, this method has limited sensitivity, with a cancer detection rate of 27%–40% and a risk of missing up to 25% of clinically significant PCa (csPCa).[8,9] Recent advances in multiparametric magnetic resonance imaging (mpMRI) have substantially improved csPCa detection through high-resolution anatomical and functional imaging. MRI-targeted biopsy (MRI-TB), fusing mpMRI findings with real-time United States (US) to guide precise sampling, demonstrates superior csPCa detection over SB while reducing diagnosis of clinically insignificant PCa (ciPCa).[10,11] Prostate Imaging Reporting and Data System (PI-RADS) version 2.1 scoring standardizes lesion characterization, with scores ≥3 indicating biopsy-eligible risk.[12]

Although the principles of MRI-TB superiority and PSAD utility are recognized, their application to individual PI-RADS categories in the PZ—a region prone to both cancer and confounding inflammation—remains inadequately defined. The aim of this study is to (1) determine the differential performance of SB, MRI-TB, and combined biopsy (CB) for each PI-RADS category; (2) quantify the category-specific prevalence and impact of chronic prostatitis (CP); and (3) validate a PSAD threshold (>0.15 ng/mL/mL) in a PZ cohort enriched with CP. We hypothesize that the diagnostic advantage of MRI-TB varies by PI-RADS category and that PSAD can effectively stratify biopsy necessity.

Methods

This single-center retrospective study received approval from the institutional ethics committee of Giresun Training and Research Hospital (ethics committee approval: KAEK-55, decision number: 08, date: 13.03.2023), with waived informed consent due to its retrospective design.

Study population

Between December 2021 and December 2024, patients who underwent mpMRI using a 1.5-Tesla MRI scanner (Magnetom Aera, Siemens Medical Solutions, Erlangen, Germany) and had lesions initially localized to the PZ with PI-RADS version 2.1 ≥3 were identified through the Picture Archiving and Communication System. A total of 223 patients underwent MRI-TB during this period, and their histopathological data were collected. The inclusion criteria were as follows: (a) a final radiological confirmation of strictly PZ-localized lesions (PI-RADS version 2.1), (b) diagnostic-quality mpMRI, and (c) both MRI-TB and 12-core TRUS-guided SB within 3 months of imaging. The exclusion criteria included the following: (1) lesions extending beyond PZ boundaries (exclusively TZ or PZ–TZ overlap) (n = 36), (2) history of previous prostate biopsy/prostate surgery (n = 19), (3) prior PCa diagnosis (n = 9), (4) inadequate mpMRI quality or missing sequences (n = 8), (5) repeat MRI-TB (n = 4), (6) absence of SB (n = 3), and (7) failure to undergo MRI-TB within 3 months of mpMRI (n = 3). TZ lesions were excluded due to higher csPCa prevalence in the PZ (70%–80%), distinct PI-RADS criteria [PZ: diffusion-weighted imaging (DWI) dominant vs. TZ: T2-weighted imaging (T2WI) dominant], and frequent BPH overlap.[2,3] The final cohort comprised 141 patients (187 PZ lesions). Figure 1 summarizes patient selection.

Image acquisition

All mpMRI examinations were performed on a 1.5T MRI system (Siemens Medical Solutions). Images were obtained with the patient in the supine position using a 16-channel pelvic phased-array coil, without an endorectal coil, in accordance with PI-RADS version 2.1 recommendations for patient comfort and feasibility at 1.5T.[12] The imaging protocol included axial/sagittal/coronal T2WI, axial T1-weighted imaging (T1WI), DWI (b-values: 0, 800, 1400 s/mm^2) with apparent diffusion coefficient (ADC) maps, and dynamic contrast-enhanced (DCE) sequences. For DCE, gadolinium-based contrast (0.1 mmoL/kg) was injected intravenously at 2–3 mL/s, followed by high-resolution three-dimensional axial T1WI every 7s for 240–300 s (slice thickness ≤3 mm). Table 1 outlines the technical parameters of the MRI sequences.

Image analysis

A single board-certified radiologist with 13 years of prostate MRI experience, blinded to histopathology, evaluated all the mpMRI scans. The interpreting radiologist had 10 years of dedicated prostate MRI experience at the commencement of the study enrollment period (December 2021). The PI-RADS version 2.1 scoring was performed prospectively as part of the initial clinical interpretation prior to biopsy. The PZ lesions were scored in accordance with the PI-RADS version 2.1 criteria, which integrate T2WI, DWI, and DCE findings for standardized characterization.[12]

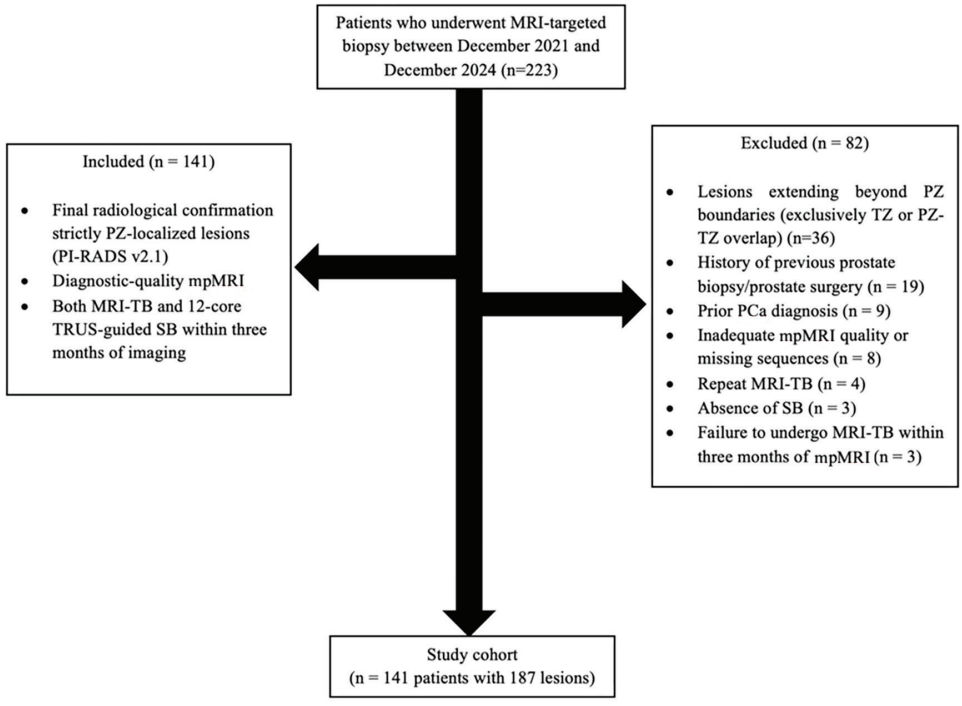

Figure 1. Flowchart of patient selection. PZ, peripheral zone; PI-RADS, Prostate Imaging Reporting and Data System; MRI-TB, magnetic resonance imaging-targeted biopsy; TRUS, transrectal ultrasound; SB, systematic biopsy; TZ, transitional zone; PCa, prostate cancer; mpMRI, multiparametric magnetic resonance imaging.

Table 1. Technical parameters for multiparametric magnetic resonance imaging acquisition

	Axial T2W	Sagittal T2W	Coronal T2W	DWI†	Axial T1W	DCE*
Sequence	TSE	TSE	TSE	EPI	GRE	3D GRE
Fat supression	No	No	No	No	Yes	Yes
TE (ms)	6.000	7.000	6.200	4.200	580	4.46
TR (ms)	108	108	108	82	13	1.72
FOV (mm)	200 × 200	200 × 200	200 × 200	260 × 260	200 × 200	260 × 260
Matrix	275 × 320	266 × 320	298 × 320	112 × 112	256 × 256	154 × 192
Slice thickness (mm)	3.5	3.5	3.5	4	3.5	3.5

†Acquired at b-values: 0, 800, 1, 400 s/mm^2 with ADC mapping.
*Dynamic acquisition: temporal resolution 7s, duration 240–300 s; gadolinium dose: 0.1 mmoL/kg at 2–3 mL/s.
ADC, apparent diffusion coefficient; DCE-MRI, dynamic contrast-enhanced magnetic resonance imaging; DWI, diffusion-weighted imaging; EPI, echo-planar imaging; FOV, field of view; GRE, gradient recalled echo; TSE, turbo spin echo; TE, echo time; TR, repetition time; T2W, T2-weighted; T1W, T1-weighted; 3D, three-dimensional.

Prostate volume and prostate-specific antigen measurement

Prostate volume was calculated from axial and sagittal T2WI using the ellipsoid formula ($\pi/6 \times AP \times$ transverse $\times$ craniocaudal diameter), as recommended by PI-RADS version 2.1.[12] All PSA values were obtained from serum samples collected within 3 months prior to the mpMRI examination, ensuring contemporaneity with the imaging findings.[13]

Magnetic resonance imaging-targeted and 12-core transrectal ultrasound-guided systematic biopsy procedure

All MRI-TB procedures were performed by two experienced radiologists (each with Two radiologists performed MRI-TB using a dedicated MRI-TRUS fusion platform (RS85 Prestige; Samsung Medison, Seoul, South Korea) and software (NavigoR v2.1; Samsung Medison, Seoul, South Korea), consistent with established technical standards.[14] Pre-procedural steps included uploading mpMRI datasets for lesion segmentation, followed by intraprocedural dual registration combining sensor-based electromagnetic tracking and organ-based deformable registration. During target sampling, ≥2 cores per lesion were obtained under continuous US guidance with real-time needle trajectory visualization, maintaining <3 mm targeting accuracy. For each patient, target lesion size was measured as the maximal axial diameter on T2WI.

Concurrently, a standardized 12-core extended sextant biopsy was performed by urologists, blinded to the MRI-TB targets, under TRUS guidance, with cores systematically obtained from six anatomical sectors per prostatic lobe: (1) the apex (medial and lateral PZ; two cores), (2) mid-gland (medial and lateral PZ; two cores), and (3) base (medial and lateral PZ; two cores), using an 18-gauge spring-loaded biopsy needle to harvest tissue cores of 15–22 mm in length, ensuring comprehensive glandular sampling for histopathological correlation.

Digital rectal examination (DRE) was performed pre-biopsy by urologists, with abnormal DRE defined as palpable nodule or glandular asymmetry. All targeted lesions

received a median of 3 cores per lesion [interquartile range (IQR): 2–5], resulting in a median total of 15 biopsy cores per patient (IQR: 14–18) when combined with the 12 systematic cores.

Histopathological analysis

Biopsy cores were evaluated by a dedicated genitourinary pathologist with 12 years of experience in prostate histopathology, in accordance with the 2014 International Society of Urological Pathology (ISUP) guidelines, including Gleason scoring and tumor involvement per core. The percentage of core involvement was used to estimate overall tumor volume, which was integrated with the Gleason score and other findings to generate a final histopathologic diagnosis for each patient. The ISUP grade groups (GGs) correspond to Gleason scores: grade 1 (3 + 3 = 6), grade 2 (3 + 4 = 7), and grade 3 (4 + 3 = 7).[15] PCa was defined as a Gleason score of ≥6 (3 + 3) (equivalent to ISUP GG ≥1); csPCa was defined as a Gleason score of ≥7 (e.g., 3 + 4 = 7, ISUP GG ≥2), an estimated tumor volume of ≥0.5 cm^3, or extraprostatic extension; ciPCa was defined as a Gleason score of 6 (3 + 3) (ISUP GG 1); and CP was diagnosed histopathologically based on the presence of a chronic inflammatory cell infiltrate within the prostatic stroma.

Reference standard and definition of outcomes

For the purpose of calculating detection rates and comparing the performance of MRI-TB and SB, the CB result was used as the reference standard, as it represents the most comprehensive histopathological assessment available for each lesion.[14,16] Although radical prostatectomy is the gold standard, its use would introduce selection bias by including only surgical candidates. We acknowledge that CB may underestimate the true prevalence of cancer due to the potential for sampling error inherent in any biopsy method; however, it represents the best available benchmark for the comparative assessment of biopsy yields in a clinical setting. A lesion was considered truly positive for csPCa if it was detected through CB (ISUP GG ≥2). The detection rate of each method was calculated against this standard. Cases where CB detected csPCa that was missed by MRI-TB or SB were considered false negatives for the respective method. Lesions with a positive MRI (i.e., assigned a PI-RADS score ≥3) but a negative CB result (benign or ciPCa) were considered false-positive MRI findings.

Statistical analysis

Statistical analyses were performed using SPSS software, version 26 (IBM Corporation, Armonk, NY, USA). Normality of data distribution was evaluated using visual methods (histograms and probability plots) and analytical tests (Kolmogorov–Smirnov and Shapiro–Wilk tests). Comparisons between two continuous variables were performed using the Mann–Whitney U test, and categorical variables were compared using the McNemar test and Fisher's exact test. A P value <0.05 was considered statistically significant.

Results

Patient and lesion characteristics

Patient demographics are summarized in Table 2. Key characteristics of the study lesions, stratified by PI-RADS score, are detailed in Table 3. Median lesion size was 14 mm (IQR: 10–18 mm). Patients underwent a median of 3 MRI-TB cores per lesion (IQR: 2–5) and 15 total cores per patient (IQR: 14–18). DRE was abnormal in 44 patients (31.2%). Histopathological assessment identified PCa in 73 patients (51.8%), stratified as clinically significant (csPCa, ISUP GG ≥2, n = 37, 26.2%) or clinically insignificant (ciPCa, ISUP GG 1, n = 36, 25.6%). Benign pathology was observed in 67 patients (47.5%), including CP in 48 cases (34.0%) (Table 4).

Overall biopsy performance

For overall PCa detection, CB demonstrated superior detection (42.8%, 80/187) to both MRI-TB (34.8%, 65/187; $P < 0.001$) and SB (26.7%, 50/187; $P < 0.001$). For csPCa (ISUP ≥2), MRI-TB (17.7%, 33/187) outperformed SB (10.7%, 20/187; $P < 0.001$), and CB (19.8%, 37/187) provided no significant additional benefit over MRI-TB alone ($P = 0.125$). Category-specific detection rates and csPCa yields across PI-RADS categories are detailed in Table 5.

Category-specific performance and International Society of Urological Pathology upgrades

Significant differences in diagnostic performance emerged across PI-RADS categories, with MRI-TB demonstrating category-specific advantages in both PCa detection and risk stratification (Table 5). Critically, among the 41 PI-RADS 3 lesions, MRI-TB identified four csPCas (ISUP GG ≥2) missed by SB,

Table 2. Demographic and clinical characteristics of the study cohort

	Value
Patients	141
Lesion of numbers	187
Age	
Mean ± SD	64.3 ± 7
Median (range)	64 (45–83)
PSA (ng/mL)	
Mean ± SD	10 ± 9.2
<4.0 ng/mL	16 (11.3%)
4.0–10.0 ng/mL	80 (56.7%)
>10.0 ng/mL	45 (32%)
Prostate volume (mL)	
Mean ± SD	72.17 ± 34.82
Median (range)	70 (13–196)
PSA density	
Mean ± SD	0.16 ± 0.17
>0.15 ng/mL/mL	48/141 (34%)*
Lesion characteristics	
Median size (mm)	14 (IQR: 10–18)
PI-RADS 3	41 (21.9%)
PI-RADS 4	92 (49.1%)
PI-RADS 5	54 (29%)
Biopsy parameters	
Median targeted cores per lesion	3 (IQR: 2–5)
Median total cores per patient	15 (IQR: 14–18)
Clinical findings	
Abnormal digital rectal examination	44 (31.2%)
Chronic prostatitis on histopathology	48 (34)

*PSAD >0.15 ng/mL/mL calculated for entire cohort.
IQR, interquartile range; PI-RADS, Prostate Imaging Reporting and Data System; PSA, prostate-specific antigen; SD, standard deviation.

yielding a csPCa detection rate of 9.8% (4/41) for MRI-TB compared with 0% (0/41) for SB. For the 92 PI-RADS 4 lesions, MRI-TB demonstrated superior csPCa detection to SB [20.7% (19/92) vs. 10.9% (10/92); $P = 0.004$]. When using CB as the reference standard, this resulted in 3 false negatives for MRI-TB vs. 12 false negatives for SB among PI-RADS 4 lesions. In lesions where both methods detected cancer (n = 17), MRI-TB upgraded the ISUP grade in 35.3% (6/17) of cases—comprising two upgrades from GG 1 to GG 2, three from GG 2 to GG 3, and one from GG 1 to GG 3—thereby altering clinical risk stratification (Figure 2). In the 54 PI-RADS 5 lesions, both methods showed equivalent csPCa detection [18.5% (10/54) each; $P = 1.000$]. Among lesions where both MRI-TB and SB detected PCa (n = 13), MRI-TB upgraded the ISUP grade in 7.7% of cases (1/13), specifically from GG 1 to GG 3 (Figure 3). Importantly, CP remained a prevalent confounding factor, observed in 22.0% (9/41) of PI-RADS 3, 22.8% (21/92) of PI-RADS 4, and 27.8% (15/54) of PI-RADS 5 lesions, and coexisted with PCa in 55.6% (5/9), 52.4% (11/21), and 33.3% (5/15) of these CP cases, respectively.

To further investigate the performance of PI-RADS 5 lesions, two post-hoc sensitivity analyses were performed. First, to address potential overscoring, we applied an additional quantitative ADC threshold of <750 $\mu m^2/s$ to define high-risk PI-RADS 5 lesions. This refined subgroup (n = 38) demonstrated a higher csPCa detection rate of 28.9% (11/38) by using CB. Second, to evaluate the impact of tumor volume, we considered high-volume Gleason score 6 (ISUP GG 1) disease (defined as ≥50% core involvement or ≥2 positive cores) as csPCa. This reclassification increased the csPCa detection rate for all PI-RADS 5 lesions from 20.4% (11/54) to 24.1% (13/54).

Clinical parameter correlations

Patients with csPCa exhibited significantly higher PSA levels (15.3 vs. 8.2 ng/mL; $P = 0.02$), smaller prostate volumes (52.4 vs. 78.6 mL; $P < 0.001$), and elevated PSAD (0.30 vs. 0.10 ng/mL/mL; $P < 0.001$). A PSAD threshold >0.15 ng/mL/mL exhibited 78% sensitivity for csPCa; this threshold was significantly more frequent in the csPCa group than in the non-csPCa group (78% vs. 18%; $P < 0.001$). No significant age difference existed between groups (Table 6).

Table 3. Characteristics of peripheral zone lesions stratified by PI-RADS score

Characteristic	PI-RADS 3 (n = 41)	PI-RADS 4 (n = 92)	PI-RADS 5 (n = 54)	*P* value
Lesion size (mm)				
Median (IQR)	10 (8–12)	13 (11–14)	17 (15–22)	<0.001
Chronic prostatitis, n (%)	9 (22.0)	21 (22.8)	15 (27.8)	0.698
PSA, ng/mL				
Median (IQR)	7.1 (5.2–9.8)	8.9 (6.0–12.0)	14.5 (9.8–21.0)	<0.001
Prostate volume, mL				
Median (IQR)	82 (65–105)	68 (50–88)	55 (40–75)	<0.001
PSAD, ng/mL/mL				
Median (IQR)	0.09 (0.06–0.12)	0.13 (0.09–0.19)	0.26 (0.17–0.40)	<0.001
PSAD >0.15, n (%)	7 (17.1)	32 (34.8)	32 (59.3)	<0.001

Statistically significant *P* values ($P < 0.05$) are shown in bold. IQR, interquartile range; PSA, prostate-specific antigen; PSAD, PSA density; PI-RADS, Prostate Imaging Reporting and Data System.

Table 4. Histopathological diagnosis of patients with PI-RADS ≥3 peripheral zone lesions

Histopathological diagnosis	Patients, n (%)
Prostate cancer	73 (51.8)
Clinically significant (ISUP GG ≥2)	37 (26.2)
Clinically insignificant (ISUP GG 1)	36 (25.6)
Atypical small acinar proliferation	1 (0.7)
Benign pathology	67 (47.5)
Chronic prostatitis	48 (34)
Benign without prostatitis	19 (13.5)
Total	141 (100)

GG, grade group; ISUP, International Society of Urological Pathology; PI-RADS, Prostate Imaging Reporting and Data System.

Table 5. Comparative detection rates of prostate cancer subtypes by biopsy method across PI-RADS categories in peripheral zone lesions

PI-RADS score		Systematic biopsy (SB) (n, %)	MRI-targeted biopsy (TB) (n, %)	Combined biopsy (CB) (n, %)	SB vs. MRI-TB *P* value	SB vs. CB *P* value	MRI-TB vs. CB *P* value
3 (n = 41)	PCa	6 (41)	16 (39.1)	17 (41.5)	0.006	0.001	1.000
	csPCa	0	4 (9.8)	4 (9.8)	0.125	0.125	1.000
	ciPca	6 (41)	12 (29.3)	13 (31.7)	–	–	–
	Benign	35 (85.4)	25 (60.9)	24 (58.5)	–	–	–
4 (n = 92)	PCa	28 (30.5)	30 (32.7)	41 (44.6)	0.839	**<0.001**	**0.001**
	csPCa	10 (10.9)	19 (20.7)	22 (23.9)	**0.004**	**<0.001**	0.25
	ciPca	18 (19.6)	11 (12)	19 (20.7)	–	–	–
	Benign	64 (69.5)	62 (67.3)	51 (55.4)	–	–	–
5 (n = 54)	PCa	16 (29.6)	19 (35.2)	22 (40.8)	0.508	0.031	0.250
	csPCa	10 (18.5)	10 (18.5)	11 (20.4)	1.000	1.000	1.000
	ciPca	6 (11.1)	9 (16.7)	11 (20.4)	–	–	–
	Benign	38 (70.4)	35 (64.8)	32 (59.2)	–	–	–

Comparisons were performed only for csPCa detection rates between biopsy methods. '–' indicates no statistical comparison performed. Statistically significant *P* values ($P < 0.05$) are shown in bold.
PI-RADS, Prostate Imaging Reporting and Data System; PCa, prostate cancer; csPCa, clinically significant prostate cancer; ciPCa, clinically insignificant prostate cancer.

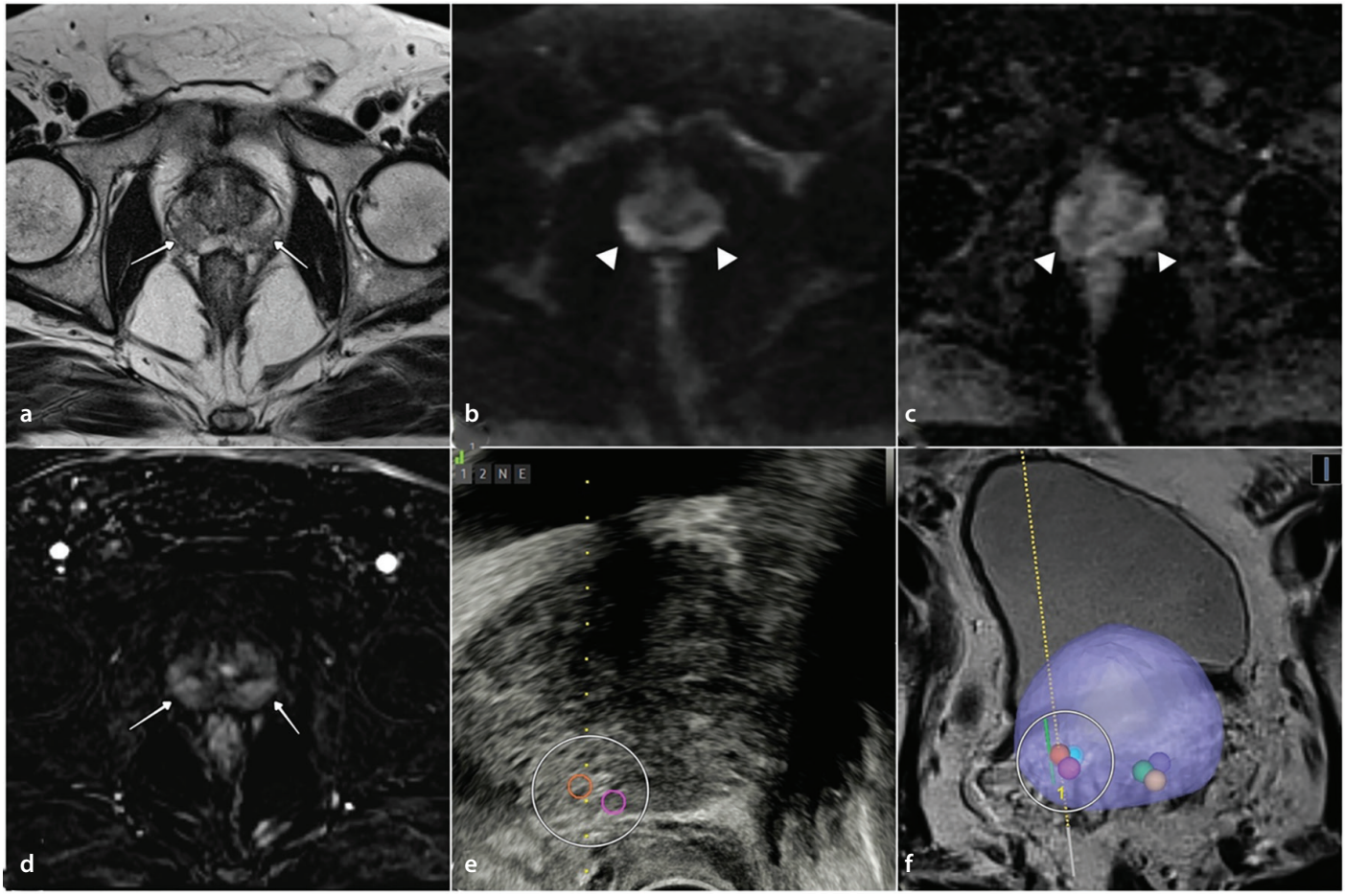

Figure 2. Multiparametric magnetic resonance imaging (MRI) and MRI-targeted biopsy (MRI-TB) findings in a 67-year-old man with bilateral PI-RADS category 4 peripheral zone (PZ) lesions. **(a)** Axial T2-weighted image demonstrates heterogeneous hypointense foci in bilateral PZs (arrows). **(b)** High b-value diffusion-weighted imaging (b = 1.400 s/mm^2) shows corresponding hyperintense signal. **(c)** Apparent diffusion coefficient map confirms diffusion restriction with hypointense signal (arrowheads). **(d)** Dynamic contrast-enhanced subtraction image reveals early arterial phase enhancement in both lesions (arrows). **(e)** Transrectal ultrasound with electromagnetic needle tracking during fusion biopsy of right PZ lesion (ring). **(f)** MRI-TB software overlay displaying co-registered bilateral targets with planned needle trajectory (ring). Histopathologic diagnosis: MRI-TB confirmed Gleason score 3 + 4 = 7 (ISUP GG 2) adenocarcinoma in both lesions. PI-RADS, Prostate Imaging Reporting and Data System; GG, grade group; ISUP, International Society of Urological Pathology.

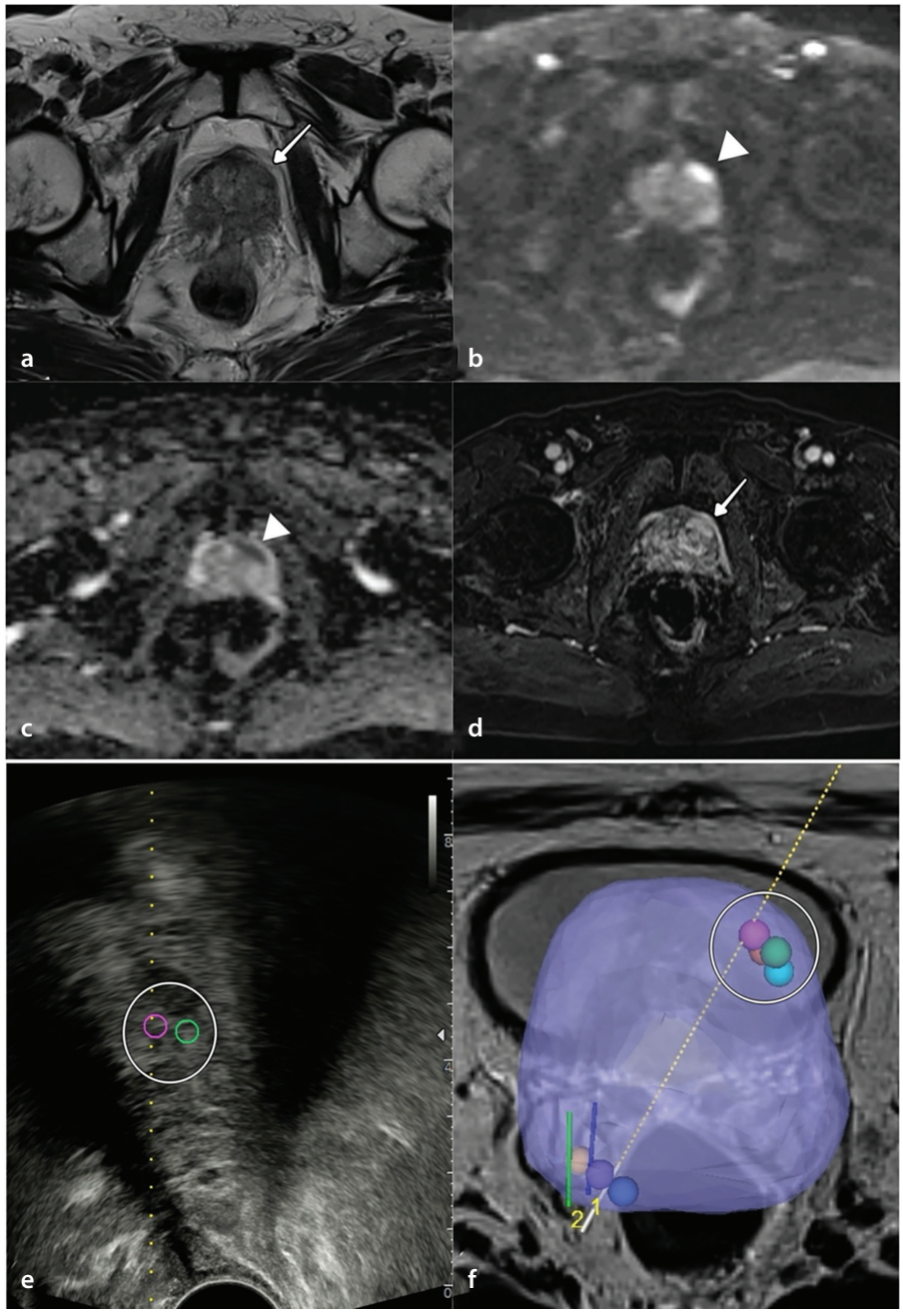

Figure 3. Multiparametric magnetic resonance imaging (MRI) and MRI-targeted biopsy (MRI-TB) of a PI-RADS category 5 peripheral zone lesion in a 75-year-old man. **(a)** Axial T2-weighted image shows a distinct hypointense focus in the left anterior peripheral zone (PZ) (arrow). **(b)** High b-value diffusion-weighted imaging (b = 1.400 s/mm^2) demonstrates marked hyperintensity. **(c)** Apparent diffusion coefficient map reveals corresponding hypointensity indicating diffusion restriction (arrowheads). **(d)** Dynamic contrast-enhanced subtraction image displays early intense arterial enhancement (arrow). **(e)** Transrectal ultrasound with electromagnetic tracking during biopsy of the left PZ target (ring). **(f)** MRI-TB fusion software overlay depicting needle trajectory registration (ring). Histopathologic diagnosis: MRI-TB confirmed Gleason score 4 + 4 = 8 (ISUP GG 4) adenocarcinoma. PI-RADS, Prostate Imaging Reporting and Data System; GG, grade group; ISUP, International Society of Urological Pathology.

Table 6. Comparative analysis of clinical parameters in patients with and without clinically significant prostate cancer (csPCa)

	csPCa (–) (n = 104, %)	csPCa (+) (n = 37, %)	*P* value
PSA (ng/mL)	8.2 ± 5.1	15.3 ± 14.2	**0.02**
Prostate volume (mL)	78.6 ± 33.7	52.4 ± 25.8	**<0.001**
PSA density (PSAD) **PSAD >0.15 ng/mL/mL**	0.10 ± 0.05 19 (18)	0.30 ± 0.25 29 (78.4)	**<0.001** **<0.001**
Age	63.8 ± 6.5	65.9 ± 8.1	0.185

Data presented as mean ± standard deviation or n (%). Statistically significant *P* values (*P* < 0.05) are shown in bold. PSA, prostate-specific antigen.

Discussion

Our study establishes that MRI-TB significantly enhances the detection of csPCa in PI-RADS ≥3 PZ lesions compared with SB, with maximal advantage observed in PI-RADS 4 lesions, where csPCa detection doubled (20.7% vs. 10.9%; $P = 0.004$). Crucially, our study addresses three critical gaps in PZ-specific diagnosis: 1) quantifying CP as a primary confounder (identified in 34.0% of benign cases), 2) demonstrating category-dependent biopsy performance across PI-RADS 3/4/5 subgroups, and 3) validating PSAD >0.15 ng/mL/mL as a robust predictor of csPCa (78% sensitivity). These findings refine biopsy pathways for the PCa-prone PZ—where 70%–80% of malignancies originate—through rigorous correlation of mpMRI features with histopathological outcomes.[2,3]

The principal novelty of our study lies in providing granular, category-specific data that refine the application of MRI-TB and PSAD for PZ lesions. We demonstrate that the diagnostic advantage of MRI-TB is maximal for PI-RADS 4 lesions, shows equipoise with SB for PI-RADS 5, and remains critical for detecting csPCa in PI-RADS 3. Furthermore, we quantitatively demonstrate that CP is a pervasive confounder not only in indeterminate (PI-RADS 3) but also in highly suspicious (PI-RADS 4–5) lesions, where it frequently coexists with cancer, thus presenting a profound diagnostic challenge. This precise stratification, combined with the validation of a PSAD >0.15 ng/mL/mL threshold in this CP-enriched cohort, provides a novel, actionable framework for personalizing biopsy decisions.

In our study, the CB approach demonstrated superior overall PCa detection (42.8% of lesions) to both MRI-TB (34.8%, $P < 0.001$) and SB (26.7%, $P < 0.001$), aligning with findings by Ahdoot et al.[14] For csPCa, MRI-TB significantly outperformed SB (17.7% vs. 10.7% of lesions; $P < 0.001$), corroborating the reported 38% vs. 26% detection advantage for MRI-TB in the study by Kasivisvanathan et al.[16] Our csPCa detection rates (SB: 10.7%; MRI-TB: 17.7%) were lower than those in high-prevalence cohorts, attributable to the following: (1) exclusion of TZ lesions with higher csPCa risk; (2) high CP prevalence (34% of benign cases), reducing specificity; and (3) a lower-risk cohort (only 32% with PSA >10 ng/mL vs. 45%–60% in other studies).[2,3,16-19] Crucially, CB provided no significant additional benefit over MRI-TB alone for csPCa detection (19.8% vs. 17.7%; $P = 0.125$), suggesting targeted sampling may suffice as a primary diagnostic method when supplemented with validated risk-stratification tools. Additionally, a meta-analysis by Schoots et al.,[9] including 16 studies and 1,926 patients, demonstrated that MRI-TB was 20% more effective than SB in detecting csPCa ($P < 0.05$), although no significant difference was noted in overall PCa detection between the two modalities. Our findings thus reinforce the superior csPCa detection of MRI-TB over SB and further confirm CB's advantage in overall PCa detection compared with SB alone.

The management of PI-RADS 3 lesions remains challenging due to their indeterminate nature. In our cohort, although the difference in csPCa detection between MRI-TB and SB in PI-RADS 3 lesions did not reach statistical significance, MRI-TB identified csPCa cases missed by SB. This highlights MRI-TB's added diagnostic value, even in lower-risk lesions, and supports its role in the diagnostic pathway for PI-RADS 3 cases. The low overall csPCa yield (9.8%) in PI-RADS 3 lesions—coupled with a 22% CP rate—further underscores the limitations of relying solely on mpMRI for indeterminate lesions. Thus, adjunctive biomarkers (e.g., PCA3, SelectMDx) or serial PSAD monitoring should be integrated to optimize risk stratification and reduce unnecessary biopsies.[17,18]

In de Braekt et al.[19] reported equivalent csPCa detection between SB and MRI-TB for PI-RADS 4 lesions ($P > 0.05$). This contrasts sharply with our findings, where MRI-TB demonstrated significantly superior csPCa detection over SB (20.7% vs. 10.9%; $P = 0.004$). The discrepancy may be attributed to key methodological differences—our cohort exclusively comprised patients who were biopsy naïve, and MRI-TB dominated csPCa detection within CB-positive cases. Crucially, the limited diagnostic advantage of MRI-TB over SB in our cohort also stems from prevalent CP (34% of benign cases), which mimics csPCa on mpMRI.

Our study reveals a critical nuance in PI-RADS 4 lesions; the limited diagnostic advantage of MRI-TB over SB (csPCa detection: 20.7% vs. 10.9%; $P = 0.004$) likely stems from prevalent CP, which constituted 34% of benign cases. This inflammatory condition mimics csPCa on mpMRI through characteristic DWI restriction and early DCE enhancement patterns, posing a major diagnostic challenge.[16,19] For such lesions, adjunctive PSAD (>0.15 ng/mL/mL) or non-focal morphology assessment are recommended to enhance specificity and reduce unnecessary biopsies.

The 26.9% prevalence of CP in our cohort (34.0% of benign cases) aligns with contemporary studies of PI-RADS ≥3 populations, confirming this reflects expected diagnostic challenges rather than cohort irregularity.[17–19] Patients with elevated PSA levels (mean: 10.03 ng/mL) and suspicious mpMRI lesions are inherently enriched for inflammatory conditions that mimic csPCa through shared imaging features—particularly diffusion restriction and early enhancement patterns on DCE sequences.[20] Furthermore, the exclusion of patients with prior biopsies likely contributed to the observed prevalence of detection of subclinical CP, as untreated inflammation accumulates over time.[1,5] Notably, the 31.2% abnormal DRE rate (44/141) correlates with both CP prevalence (26.9%) and contemporary MRI-TB studies, suggesting palpable glandular irregularities may reflect underlying inflammatory changes that confound mpMRI interpretation.[21,22]

For PI-RADS 5 lesions, the equivalent csPCa detection rates between SB and MRI-TB (18.5% each; $P = 1.000$) indicate comparable efficacy for large, conspicuous lesions (median size: 17 mm, IQR: 15–22 mm). However, our overall csPCa detection rate for PI-RADS 5 lesions (20.4% by CB) is lower than the very high rates (60%–90%) often reported in the literature.[16,19,21] This critical discrepancy can be attributed to several factors inherent to our study cohort: (1) the exclusion of TZ cancers, which frequently present as aggressive PI-RADS 5 tumors; (2) the high prevalence of CP (27.8%); and (3) nearly 40% of lesions having a PSAD below the 0.15 ng/mL/mL threshold, suggesting a less aggressive profile. Therefore, although PI-RADS 5 remains a high-risk category, its predictive value is not absolute and is substantially influenced by the underlying prevalence of confounding inflammation and the specific risk profile of the patient population. This aligns with the findings of In de Braekt et al.[19] but contrasts with studies reporting MRI-TB superiority.[21,22] In our cohort, 27.8% of PI-RADS 5 lesions showed imaging features consistent with CP, complicating lesion characterization. Technical heterogeneity in MRI acquisition, interpretation variability, operator experience, or biopsy targeting accuracy may underlie these discrepancies. Consequently, for morphologically overt PI-RADS 5 PZ lesions (≥15 mm), systematic sampling may achieve comparable csPCa detection to targeted ap-

proaches, potentially optimizing resource utilization in high-volume settings. Nevertheless, the 27.8% CP prevalence remains a critical confounder for mpMRI specificity.[20]

To address the potential for overscoring and refine the predictive value of PI-RADS 5 lesions, two post-hoc sensitivity analyses were performed. Our post-hoc sensitivity analyses offer potential pathways to refine the predictive value of PI-RADS 5 lesions. The application of a quantitative ADC threshold (<750 μm²/s) successfully identified a subgroup with a higher csPCa yield (28.9%), suggesting that incorporating quantitative metrics can help distinguish the highest-risk lesions within this category. Furthermore, considering high-volume Gleason 6 disease as clinically significant increased the overall csPCa detection rate to 24.1%, highlighting that a subset of these tumors may have greater clinical relevance than traditionally assigned. These exploratory analyses emphasize that beyond the qualitative PI-RADS 5 score, adjunctive quantitative and volumetric parameters could enhance risk stratification and clinical decision-making.

Regarding differential csPCa detection across PI-RADS categories, our data revealed two key patterns. First, for PI-RADS 4 lesions, CB detected significantly more csPCa than SB alone (23.9% vs. 10.9%; $P < 0.001$) and marginally more than MRI-TB alone (23.9% vs. 20.7%; $P = 0.25$). This three-case increment (22 vs. 19 lesions) reflects CB's capacity to sample both MRI-suspicious foci and occult csPCa outside targets. Importantly, contemporary evidence indicates that SB detects csPCa in approximately 10% of cases within MRI-normal contralateral lobes, reinforcing SB's role in comprehensive sampling despite negative mpMRI findings.[23] Prior studies confirm that 10%–15% of csPCa is MRI invisible but is detected by random sampling, particularly in glands with heterogeneous backgrounds such as CP.[16,19] Second, in PI-RADS 5 lesions, equivalent csPCa detection by SB and MRI-TB (18.5% each; $P = 1.000$) was observed. This equivalence likely stems from their conspicuous size (median 17 mm, IQR: 15–22 mm), enabling comparable sampling efficacy for both methods. Notably, 27.8% of these lesions exhibited concurrent CP, potentially contributing to false-positive MRI interpretations.[20]

Our findings validate PSAD as a pivotal discriminator for csPCa, with 78% of patients with csPCa exhibiting PSAD > 0.15 ng/mL/mL versus 18% in non-csPCa cases ($P < 0.001$). This aligns with prior evidence that PSAD enhances specificity in PI-RADS 4 lesions, where CP mimics malignancy.[17,20] The inverse correlation between prostate volume and csPCa risk (csPCa: 52.4 vs. non-csPCa: 78.6 mL; $P < 0.001$) further supports volumetric assessment in biopsy decisions. Although PSA was elevated in csPCa (15.3 vs. 8.2 ng/mL; $P = 0.02$), its overlap with inflammatory conditions (e.g., CP) limits standalone utility. We advocate integrating PSAD >0.15 ng/mL/mL into MRI-TB workflows to avoid unnecessary biopsies in equivocal PI-RADS 3–4 lesions.[17,24]

Although age is a well-established risk factor for PCa,[1,25] our study found no statistically significant difference between the cancer and non-cancer groups (median: 65 vs. 63.5 years; $P > 0.05$). This may reflect cohort-specific characteristics—nearly half the patients (49.7%) were aged 61–70 years, with balanced distribution between groups. Potential explanations include the relatively narrow age range, limited sample size for subgroup analyses, or selection bias from exclusively including PI-RADS ≥3 cases. Nevertheless, the established role of age in PCa risk stratification remains unchallenged in broader populations.[26]

Our study has several limitations requiring acknowledgment. First, its retrospective, single-center design and exclusive focus on PZ lesions may introduce selection bias, partially explaining lower csPCa rates than in studies including TZ cancers or high-PSA cohorts.[2,3,15,18] Second, the use of CB as the reference standard (as detailed under Methods) may affect accuracy estimates for MRI-invisible cancers, although this is a recognized limitation in biopsy comparison studies.[13–15,25] Additionally, tumor volume was estimated from core biopsy specimens rather than measured from radical prostatectomy specimens. Although this is a standard methodology for pre-treatment risk stratification, it remains an estimation subject to sampling error. Third, we did not stratify lesions by specific PZ location; thus, the advantage of MRI-TB over SB may be underestimated for under-sampled regions. The absence of this location-specific analysis limits the granularity of our conclusions regarding the differential advantage of MRI-TB. Future prospective studies designed to include such detailed anatomical mapping are warranted to provide more specific guidance. Fourth, reliance on a single radiologist for PI-RADS scoring precludes assessment of inter-observer variability. Fifth, although PI-RADS version 2.1 recommends 3T MRI, diagnostic accuracy for PI-RADS ≥3 PZ lesions is comparable at 1.5T with modern sequences; however, exclusive use of a pelvic phased-array coil (without endorectal coil) could reduce spatial resolution for sub-centimeter lesions—a limitation mitigated by our cohort's median lesion size.[13] Sixth, performing SB after MRI-TB may introduce hemorrhage-related sampling bias. Seventh, the transrectal biopsy approach, although appropriate for posteriorly located PZ lesions, contrasts current guideline recommendations favoring transperineal methods to reduce sepsis risk.[13,27] Finally, the high CP prevalence remains a key confounder for PI-RADS specificity, underscoring the need for future integration of quantitative imaging biomarkers (e.g., ADC histogram analysis) to improve discrimination.[18,21]

In conclusion, our study provides a refined, evidence-based algorithm for prostate biopsy in patients with PZ lesions, moving beyond broad principles to deliver category-specific guidance. We establish that the diagnostic advantage of MRI-TB is not uniform but is maximized for PI-RADS 4 lesions, whereas it is equivalent to SB for large, conspicuous PI-RADS 5 lesions. The high prevalence of CP (34% of benign cases) is a major confounder across all categories, frequently mimicking csPCa and reducing mpMRI specificity. Furthermore, we validate a PSAD threshold of >0.15 ng/mL/mL as a pivotal tool for risk stratification. These findings support using MRI-TB alone for PI-RADS ≥4 lesions or in patients with elevated PSAD, reserving CB for equivocal PI-RADS 3–4 cases. The high rate of inflammatory mimics underscores the critical need for integrating adjunctive biomarkers to improve specificity in the future.

Footnotes

Conflict of interest disclosure

The authors declared no conflicts of interest.

References

1. Siegel RL, Giaquinto AN, Jemal A. Cancer statistics, 2024. *CA Cancer J Clin.* 2024;74(1):12-49. [Crossref]
2. Yacoub JH, Oto A. MR imaging of prostate zonal anatomy. *Radiol Clin North Am.* 2018;56(2):197-209. [Crossref]
3. Lee CH, Akin-Olugbade O, Kirschenbaum A. Overview of prostate anatomy, histology, and pathology. *Endocrinol Metab Clin North Am.* 2011;40(3):565-575, viii-ix. [Crossref]
4. Madersbacher S, Alcaraz A, Emberton M, et al. The influence of family history on prostate cancer risk: implications for clinical management. *BJU Int.* 2011;107(5):716-721. [Crossref]

5. Roddam AW, Duffy MJ, Hamdy FC, et al. Use of prostate-specific antigen (PSA) isoforms for the detection of prostate cancer in men with a PSA level of 2-10 ng/mL: systematic review and meta-analysis. *Eur Urol.* 2005;48(3):386-99; discussion 398-399. [Crossref]
6. Huang Y, Li ZZ, Huang YL, Song HJ, Wang YJ. Value of free/total prostate-specific antigen (f/t PSA) ratios for prostate cancer detection in patients with total serum prostate-specific antigen between 4 and 10 ng/mL: a meta-analysis. *Medicine (Baltimore).* 2018;97(13):e0249. [Crossref]
7. Benson MC, Whang IS, Pantuck A, et al. Prostate specific antigen density: a means of distinguishing benign prostatic hypertrophy and prostate cancer. *J Urol.* 1992;147(3 Pt 2):815-816. [Crossref]
8. Omer A, Lamb AD. Optimizing prostate biopsy techniques. *Curr Opin Urol.* 2019;29(6):578-586. [Crossref]
9. Schoots IG, Roobol MJ, Nieboer D, Bangma CH, Steyerberg EW, Hunink MG. Magnetic resonance imaging-targeted biopsy may enhance the diagnostic accuracy of significant prostate cancer detection compared to standard transrectal ultrasound-guided biopsy: a systematic review and meta-analysis. *Eur Urol.* 2015;68(3):438-450. [Crossref]
10. Brown AM, Elbuluk O, Mertan F, et al. Recent advances in image-guided targeted prostate biopsy. Abdom Imaging. 2015;40(6):1788-1799. [Crossref]
11. Gaziev G, Wadhwa K, Barrett T, et al. Defining the learning curve for multiparametric magnetic resonance imaging (MRI) of the prostate using MRI-transrectal ultrasonography (TRUS) fusion-guided transperineal prostate biopsies as a validation tool. *BJU Int.* 2016;117(1):80-86. [Crossref]
12. Turkbey B, Rosenkrantz AB, Haider MA, et al. Prostate imaging reporting and data system version 2.1: 2019 update of prostate imaging reporting and data system version 2. *Eur Urol.* 2019;76(3):340-351. [Crossref]
13. Cornford P, van den Bergh RCN, Briers E, et al. EAU-EANM-ESTRO-ESUR-ISUP-SIOG Guidelines on Prostate Cancer-2024 Update. Part I: Screening, Diagnosis, and Local Treatment with Curative Intent. *Eur Urol.* 2024;86(2):148-163. [Crossref]
14. Ahdoot M, Wilbur AR, Reese SE, et al. MRI-targeted, systematic, and combined biopsy for prostate cancer diagnosis. *N Engl J Med.* 2020;382(10):917-928. [Crossref]
15. Epstein JI, Egevad L, Amin MB, et al. The 2014 International Society of Urological Pathology (ISUP) consensus conference on gleason grading of prostatic carcinoma: definition of grading patterns and proposal for a new grading system. *Am J Surg Pathol.* 2016;40(2):244-252. [Crossref]
16. Kasivisvanathan V, Rannikko AS, Borghi M, et al. MRI-targeted or standard biopsy for prostate-cancer diagnosis. *N Engl J Med.* 2018;378(19):1767-1777. [Crossref]
17. Görtz M, Radtke JP, Hatiboglu G, et al. The value of prostate-specific antigen density for prostate imaging-reporting and data system 3 lesions on multiparametric magnetic resonance imaging: a strategy to avoid unnecessary prostate biopsies. *Eur Urol Focus.* 2021;7(2):325-331. [Crossref]
18. Brizmohun Appayya M, Sidhu HS, Dikaios N, et al. Characterizing indeterminate (Likert-score 3/5) peripheral zone prostate lesions with PSA density, PI-RADS scoring and qualitative descriptors on multiparametric MRI. *Br J Radiol.* 2018;91(1083):20170645. [Crossref]
19. In de Braekt T, van Rooij SBT, Daniels-Gooszen AW, et al. Accuracy of MRI-ultrasound fusion-guided and systematic biopsy of the prostate. *Br J Radiol.* 2024;97(1158):1132-1138. [Crossref]
20. Ullrich T, Arsov C, Quentin M, et al. Analysis of PI-RADS 4 cases: management recommendations for negatively biopsied patients. *Eur J Radiol.* 2019;113:1-6. [Crossref]
21. Liu Y, Wang S, Xu G, et al. Effectiveness and accuracy of MRI-ultrasound fusion targeted biopsy based on PI-RADS v2.1 category in transition/peripheral zone of the prostate. *J Magn Reson Imaging.* 2023;58(3):709-717. [Crossref]
22. Nativ O, Shefler A, Bejar J, et al. Performance of standard systematic biopsy versus MRI/TRUS fusion biopsy using the Navigo® system in contemporary cohort. *Urol Oncol.* 2024;42(5):159.e1-159.e7. [Crossref]
23. Pepe P, Pepe L, Fiorentino V, Curduman M, Fraggetta F. Multiparametric MRI targeted prostate biopsy: when omit systematic biopsy? *Arch Ital Urol Androl.* 2024;96(4):12992. [Crossref]
24. Distler FA, Radtke JP, Bonekamp D, et al. The value of PSA density in combination with PI-RADS™ for the accuracy of prostate cancer prediction. *J Urol.* 2017;198(3):575-582. [Crossref]
25. Zhou CK, Check DP, Lortet-Tieulent J, et al. Prostate cancer incidence in 43 populations worldwide: an analysis of time trends overall and by age group. *Int J Cancer.* 2016;138(6):1388-400. [Crossref]
26. Fiorentino V, Pepe L, Zuccalà V, et al. Gleason score down and upgrading at radical prostatectomy in targeted vs. systematic prostate biopsy: findings from an institutional cohort. *Pathol Res Pract.* 2025;271:156040. [Crossref]
27. Greer MD, Brown AM, Shih JH, et al. Accuracy and agreement of PIRADSv2 for prostate cancer mpMRI: a multireader study. *J Magn Reson Imaging.* 2017;45(2):579-585. [Crossref]